Multi-parameter fusion algorithm for auto focus

Jun Luo (罗 钧)*, Li Sun (孙 力), Kesong Wu (吴克松), Weimin Chen (陈伟民), and Li Fu (付 丽)

Key Laboratory of Optoelectronic Technology and System, Ministry of Education, Chongqing University, Chongqing 400030, China

**E-mail: luojun@cqu.edu.cn*

Received January 6, 2010

A multi-parameter fusion algorithm (MPFA) for auto-focus (AF) is discussed. The image sharpness evaluation algorithm (ISEA) and zoom tracking method (ZTM) are combined for AF. The zoom motor position (z) and background complexity (c) are regarded as the main parameters of this algorithm. A priority table depending on z and c is proposed. Modified ISEA or ZTM is adopted according to the priority table value. The hardware implementation of the MPFA on Texas Instruments' Davinci digital signal processor is also provided. Results show that the proposed scheme provides faster focusing compared with the conventional approaches.

OCIS codes: 000.3110, 040.1490, 110.2960, 110.5200.
doi: 10.3788/COL20100806.0580.

At present, zoom lenses have been utilized widely in various industrial applications. Auto-focus (AF) algorithm is an important factor in determining the imaging quality of a digital still camera (DSC)[1−3]. There are two ways to implement AF, namely, active AF and passive AF. In literature, only passive AF methods have been discussed, although some conventional passive AF methods have been introduced. In this letter, we introduce a new AF approach, the multi-parameter fusion algorithm (MPFA), which merges the image sharpness evaluation algorithm (ISEA) and the zoom tracking method (ZTM) according to a priority table. The priority table is based on zoom motor position (z) and background complexity (c). Results show that the MPFA provides higher focusing speed compared with conventional methods.

There are two prevalent methods used in realizing passive AF: ISEA and ZTM[4], and each has many algorithms, including sharpness evaluation operators, look-up table, geometric, and adaptive zoom tracking. However, these algorithms have several general drawbacks. Firstly, a complex background image results in local peak values of the image definition. In addition, more time is required in searching for the maximum definition value when using ISEA[5−14]. Secondly, the look-up table method uses a large amount of memory, and no mechanism is provided to select the right trace curve when the zoom motor is moved towards the tele-angle direction; this is due to the one-to-many mapping problem. Thirdly, in the geometric ZTM, offset between the estimated trace curve and true trace curve gradually increases for the zoom motor positions towards the tele-angle direction. Fourthly, the adaptive ZTM improves the tracking accuracy at the expense of tracking speed[4]. Thus, a more effective AF approach is necessary. The new MPFA presented in this letter can solve these problems in various ways.

There are numerous evaluation functions for digital image sharpness, including variance operator, power gradient operator, and Laplacian operator. The performance of each operator is different in relation to focusing speed.

The output of high-pixel color charge-coupled device/complementary metal-oxide semiconductor (CCD/CMOS) image sensors are RAW format image data. In conventional methods, data are restored in BMP or JPEG formats, the color space conversion is taken, and image definition is evaluated via luminance or green (G) component. However, these methods are not so efficient that they require a large quantity of calculation and are also time-consuming.

According to the above discussion, the gradient operator model, which is directly based on RAW format, is provided by

$$F = \sum_{\mathrm{mat}_x} \sum_{\mathrm{mat}_y} (f_x^2(\mathrm{mat}_x, \mathrm{mat}_y) + f_y^2(\mathrm{mat}_x, \mathrm{mat}_y)), \quad (1)$$

where

$$g(\mathrm{mat}_x, \mathrm{mat}_y) = 0.299 \times R(\mathrm{mat}_x, \mathrm{mat}_y) + 0.587 \times G'(\mathrm{mat}_x, \mathrm{mat}_y) + 0.114 \times B(\mathrm{mat}_x, \mathrm{mat}_y), \quad (2)$$

$$f_x(\mathrm{mat}_x, \mathrm{mat}_y) = g(\mathrm{mat}_{x+1}, \mathrm{mat}_y) - g(\mathrm{mat}_x, \mathrm{mat}_y), \quad (3)$$

$$f_y(\mathrm{mat}_x, \mathrm{mat}_y) = g(\mathrm{mat}_x, \mathrm{mat}_{y+1}) - g(\mathrm{mat}_x, \mathrm{mat}_y). \quad (4)$$

In the above expressions, "mat" is a MAT unit, which has one red (R) element, two G elements, and one blue (B) element in the RAW format image acquired. In addition, $(\mathrm{mat}_x, \mathrm{mat}_y)$ is the MAT unit with coordinate (x, y), F is the focus value, $g(\mathrm{mat}_x, \mathrm{mat}_y)$ is the gray value in $(\mathrm{mat}_x, \mathrm{mat}_y)$, and $G'(\mathrm{mat}_x, \mathrm{mat}_y)$ is the average of the two G-components in $(\mathrm{mat}_x, \mathrm{mat}_y)$.

The detailed gradient operator based on RAW format is not presented here. When obtaining the focus value of each frame according to Eq. (1), hill-climbing algorithm is used to find the in-focus position.

ZTM depends on the zoom motor positions and the focus motor positions conjointly[15−18]. Figure 1 illustrates the ZTM system. Cam mechanism is adjusted by zoom motor to change the combination focal length f of 1G and 2G lens units. Zoom PI and focus PI represent

the signals of zoom lens position and focus lens position, respectively. Hence, in order to obtain clear image from the sensor, the image distance v must be adjusted to meet the imaging formula for a given object distance. In this respect, the position of the image sensor is not easy to change, but the position of the 3G lens is often changed to implement auto focus. Thus, once the combination focal length f of 1G and 2G lens units is changed, a unique in-focus plane correspondence will be obtained.

A group of zoom tracking curves comprises each scene. A scene consists of the following modes: macro, middle focus, and far focus. Differences exist among the three modes. The trace curves can be obtained through the following steps. The object distance is d_k and the zoom motor position is z_i. Conventional AF method is used to obtain the in-focus image, and the position of focus motor $f_{d_k}(z_i)$ is recorded. In this method, focus motor positions are obtained from z_{wide} to z_{tele}. Trace curve with object distance d_k is also obtained. Consequently, trace curves in different object distances are obtained. Figure 2 shows the results of this method.

The software flow chart of ZTM is shown in Fig. 3. In this chart, the key component is in-focus motor position estimation. Thus, it is critical to obtain the zoom tracking curves accurately and objectively. However, when the trace curves are in the nonlinear region, choosing the right trace curve is difficult and time-consuming.

As mentioned above, both ISEA and ZTM have flaws. Thus, a new AF method, the MPFA, is presented.

When sharpness evaluation algorithm is used, finding the in-focus plane takes more time particularly when the background image is complex. ZTM suffers from inaccuracy especially when the zoom motor position is moved towards the tele-angle direction, i.e., it is more than z_{b},

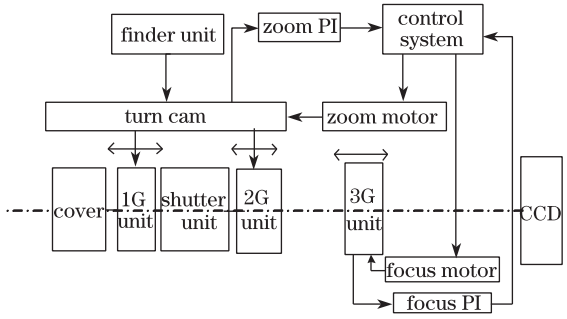

Fig. 1. ZTM system.

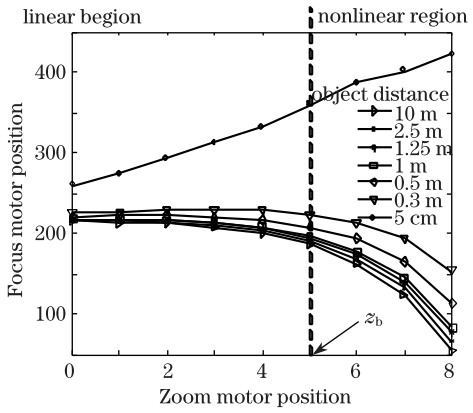

Fig. 2. Zoom tracking curve.

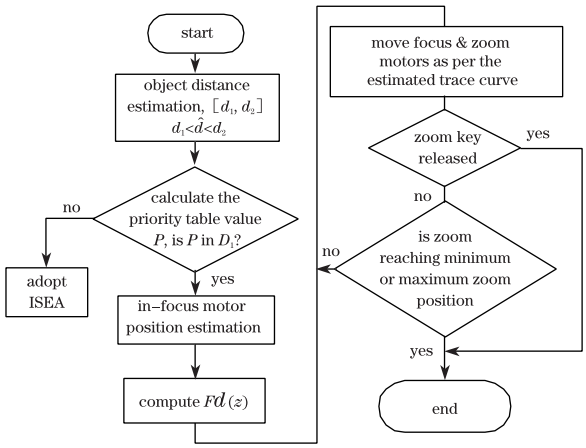

Fig. 3. Conventional ZTM software flow.

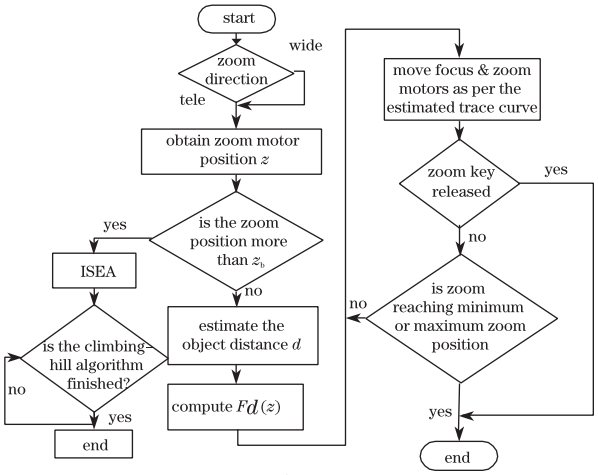

Fig. 4. MPFA software flow.

which represents the boundary position between the linear and nonlinear regions of the trace curves. When $z \geq z_{\text{b}}$, the trace curve is nonlinear. z and c are combined in the MPFA, and the software flow is illustrated in Fig. 4. To decide which approach should be used in the process of AF, z was obtained by zoom PI first, and the obtained zoom motor positions were sorted in ascending order: $\{z_1, z_2, z_3, z_4, z_5, \cdots\}$. The complexity of the background was then calculated according to the image acquired. The values $\{c_1, c_2, c_3, c_4, c_5, \cdots\}$ represent the sorted c in descending order. Here, c is the ratio between k and the number of adjacent pixels:

$$c = \frac{k}{2MN - M - N}. \tag{5}$$

where k is the number of the two adjacent pixels which have been changed; M and N denote the length and width of computing window of the image, the number of the two adjacent pixels is thus given by$M \times (N-1) + N \times (M-1) = 2MN - M - N$.

As defined above, c has two properties: 1) $0 \leq c \leq 1$, and 2) larger c corresponds to larger complexity of image, and *vice versa*.

A priority table was designed based on z and c (Fig. 5). The region determined by z and c was divided into two parts: D_1 and D_2. ZTM was adopted for AF in D_1, and ISEA was adopted in D_2. Consequently, the advantages of each method were fully utilized, and the disadvantages were avoided.

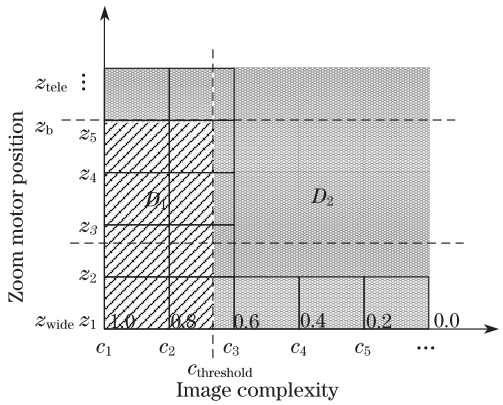

Fig. 5. Design of priority table for the AF algorithm.

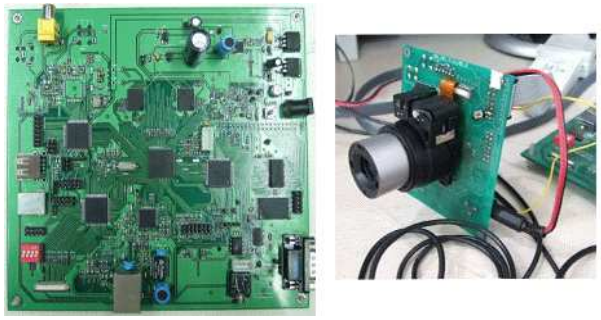

Fig. 6. Picture of the developed hardware platform based on TMS320DM6446.

Each acquired frame corresponded to a priority table value P stated in

$$\left.\begin{array}{l} P = P(c, z) \\ 0 \le c \le 1 \\ z_1 \le z \le z_N \end{array}\right\}. \tag{6}$$

The value of P based on z and c was determined by imaging system, and the right method for AF was chosen.

In Fig. 5, z is the current position of the zoom motor, z_{tele} is the zoom lens position of tele-angle, z_{wide} is the zoom lens position of wide-angle, z_{b} is the boundary zoom position, and $c_{\text{threshold}}$ is the threshold value of c. $c_{\text{threshold}}$ was also determined using our platform. When $z \le z_{\text{b}}$ and $c \ge c_{\text{threshold}}$, that is, the value of priority table P is in D_1, the image is too complex so that ZTM should be chosen. When $z \ge z_{\text{b}}$ or $c \le c_{\text{threshold}}$, that is, P is in D_2, ISEA should be chosen.

A hardware implementation of the proposed MPFA is presented by applying a typical DSC platform. The platform applied Texas Instruments' TMS320DM6446 digital media processor, image sensor, and lens head (Fig. 6).

In order to verify the focusing speed of the MPFA, we acquire 50 scenes from the object distance of 5 m and 50 scenes from 50 cm by ISEA, ZTM, and the MPFA. The maximum time consumption of the MPFA is given in Table 1, which also shows the four parts comprising time consumption. Table 2 shows the average time consumption of each method and MPFA performance compared with those of the conventional AF algorithms (ISEA and ZTM) in terms of focusing speed. The results show that the proposed MPFA provides faster focusing compared with the conventional methods.

Table 1. Time Consumption of the MPFA

Item	Time Consumption
Zoom Tracking Time	max = $16t^*$
Fine Scan Time	$1.5t$
Definition Computing Time	78 ms
Focusing Time	max = $0.5t$

$^*t$ is determined by the speed of the minisize stepper motor, and the system is used in $t \approx 100$ ms.

Table 2. Computational Performance of the Three Approaches

Approach	Required Time (ms)
ISEA	2352
ZTM	1960
MPFA	1878

In conclusion, a MPFA combining ISEA and ZTM is presented for AF. The zoom motor position and background complexity are the main parameters of this algorithm. A priority table based on these parameters is proposed to choose MPFA or ZTM for AF. Hardware implementation of the MPFA is provided. It is shown that the proposed scheme provides faster focusing compared with the conventional approaches.

This work was supported by the Key Project of the Defense and Military Metrology, the Eleventh Five-Year Plan Support of the Commission of Science Technology and Industry for National Defence (No. B20301118), and the Key Project of the Science and Technology Foundation of the Chongqing Information Industry Bureau (No. 200113013).

References

1. Y. Liu, C. Sui, and B. Li, Acta Opt. Sin. (in Chinese) **28,** 1124 (2008).
2. L. Zhao, W. Jin, Y. Chen, and B. Su, Acta Opt. Sin. (in Chinese) **28,** 1703 (2008).
3. C. Yu, B. Chang, and D. Wei, Chin. Opt. Lett. **6,** 502 (2008).
4. V. Peddigari and N. Kehtarnavaz, IEEE Trans. Consumer Electron. **51,** 1051 (2005).
5. Y. Song and M. Li, in *Proceedings of the 2006 IEEE International Conference on Mechatronics and Automation* 1237 (2006).
6. S.-M. Sohn, S.-H. Yang, S.-W. Kim, K.-H. Baek, and W.-H. Paik, IEEE Trans. Consumer Electron. **52,** 10 (2006).
7. L. Li, Q. Zeng, and F. Meng, Chin. Opt. Lett. **6,** 827 (2008).
8. R. Fu, F. Shao, G. Jiang, and M. Yu, Chin. Opt. Lett. **6,** 654 (2008).
9. C.-H. Shen and H. H. Chen, in *Proceedings of International Conference on Consumer Electronics* 69 (2006).
10. F. Li and H. Jin, in *Proceedings of the Fourth International Conference on Machine Learning and Cybernetics* 5001 (2005).
11. Q. Li, H. Feng, Z. Xu, M. Bian, S. Shen, and R. Dai, Acta. Photon. Sin. (in Chinese) **31,** 736 (2002).

12. N. Kehtarnavaz and H.-J. Oh, Real-Time Imaging **9,** 197 (2003).
13. C. Weerasinghe, M. Nilsson, S. Lichman, and I. Kharitonenko, IEEE Trans. Consumer Electron. **50,** 777 (2004).
14. T.-K. Kim, J.-S. Sohn, S.-H. Lee, K.-R. Kwon, and D.-G. Kim, in *Proceedings of 2006 IEEE International Conference on Acoustics, Speech and Signal Processing* **3,** 1188 (2006).
15. M. Sun, G. Zong, D. Dong, and J. Shi, Acta Opt. Sin. (in Chinese) **28,** 1117 (2008).
16. Y. He, J. Cui, T. Tan, and Y. Wang, in *Proceedings of the 18th International Conference on Pattern Recognition* **4,** 557 (2006).
17. J.-S. Lee, S.-J. Ko, Y. Kim, and A. Morales, in *Proceedings of International Conference on Consumer Electronics* 56 (2002).
18. Y. Kim, J.-S. Lee, A. W. Morales, and S.-J. Ko, IEEE Trans. Consumer Electron. **48,** 428 (2002).